AMERICAN SOCIETY FOR MICROBIOLOGY | Applied and Environmental Microbiology

HipH Catalyzes the Hydroxylation of 4-Hydroxyisophthalate to Protocatechuate in 2,4-Xylenol Catabolism by *Pseudomonas putida* NCIMB 9866

Hong-Jun Chao,[a] Yan-Fei Chen,[a] Ti Fang,[a] Ying Xu,[b] Wei E. Huang,[c] Ning-Yi Zhou[a,b]

Key Laboratory of Agricultural and Environmental Microbiology, Wuhan Institute of Virology, Chinese Academy of Sciences, Wuhan, People's Republic of China[a]; State Key Laboratory of Microbial Metabolism and School of Life Sciences & Biotechnology, Shanghai Jiao Tong University, Shanghai, People's Republic of China[b]; Department of Engineering Science, University of Oxford, Oxford, United Kingdom[c]

In addition to growing on *p*-cresol, *Pseudomonas putida* NCIMB 9866 is the only reported strain capable of aerobically growing on 2,4-xylenol, which is listed as a priority pollutant by the U.S. Environmental Protection Agency. Several enzymes involved in the oxidation of the *para*-methyl group, as well as the corresponding genes, have previously been reported. The enzyme catalyzing oxidation of the catabolic intermediate 4-hydroxyisophthalate to the ring cleavage substrate protocatechuate was also purified from strain NCIMB 9866, but its genetic determinant is still unavailable. In this study, the gene *hipH*, encoding 4-hydroxyisophthalate hydroxylase, from strain NCIMB 9866 was cloned by transposon mutagenesis. Purified recombinant HipH-His$_6$ was found to be a dimer protein with a molecular mass of approximately 110 kDa. HipH-His$_6$ catalyzed the hydroxylation of 4-hydroxyisophthalate to protocatechuate with a specific activity of 1.54 U mg^{-1} and showed apparent K_m values of 11.40 ± 3.05 μM for 4-hydroxyisophthalate with NADPH and 11.23 ± 2.43 μM with NADH and similar K_m values for NADPH and NADH (64.31 ± 13.16 and 72.76 ± 12.06 μM, respectively). The identity of protocatechuate generated from 4-hydroxyisophthalate hydroxylation by HipH-His$_6$ has also been confirmed by high-performance liquid chromatography and mass spectrometry. Gene transcriptional analysis, gene knockout, and complementation indicated that *hipH* is essential for 2,4-xylenol catabolism but not for *p*-cresol catabolism in this strain. This fills a gap in our understanding of the gene that encodes a critical step in 2,4-xylenol catabolism and also provides another example of biochemical and genetic diversity of microbial catabolism of structurally similar compounds.

The compound 2,4-xylenol (2,4-dimethylphenol), one of the six isomers of xylenol, is derived from cresylic acid or the tar acid fraction of coal tar. It is listed as a priority pollutant by the U.S. Environmental Protection Agency because of its environmental toxicity. Given the potential of 2,4-xylenol to cause harm to human health, including severe irritation of the skin and eyes and damage to the liver and kidneys, much interest has been focused on the understanding of its degradation by microorganisms. So far, several bacterial strains have been isolated for the transformation of 2,4-xylenol, such as *Pseudomonas* sp. (1), *Pseudomonas putida* NCIMB 9866 (2), *Paracoccus* sp. strain U120 (3), *P. putida* EKII (4), and *Alcaligenes eutrophus* JMP 134 (5, 6). Of these strains, only U120 is able to mineralize 2,4-xylenol under anaerobic conditions (3). Nevertheless, *P. putida* NCIMB 9866 is the only reported microorganism capable of mineralization of 2,4-xylenol under aerobic conditions (2).

The early studies of 2,4-xylenol catabolism by *P. putida* NCIMB 9866 in the 1960s found that it was initiated by oxidation of the *para*-methyl group to a carboxyl group, forming 4-hydroxy-3-methylbenzoate via two putative intermediates of 4-hydroxy-3-methylbenzyl alcohol and 4-hydroxy-3-methylbenzaldehyde. The *ortho*-methyl group in 4-hydroxy-3-methylbenzoate was then also oxidized to a carboxyl group, via two putative intermediates of its corresponding alcohol and aldehyde, to produce 4-hydroxyisophthalate (4COOH$_2$). 4COOH$_2$ was converted to protocatechuate (PCA), entering the *ortho* ring cleavage pathway for further metabolism (Fig. 1A) (2).

Recently, plasmid-borne *pchC*- and *pchF*-encoded *p*-cresol methylhydroxylase and *pchA*-encoded *p*-hydroxybenzaldehyde dehydrogenase in *p*-cresol catabolism were found to be responsible for the oxidation of the *para*-methyl group of 2,4-xylenol catabolism to 4-hydroxy-3-methylbenzoate (Fig. 1) (7). Besides, 4-hydroxy-3-methylbenzoate hydroxylase, which is responsible for oxidation of the *ortho*-methyl group of 2,4-xylenol to 4COOH$_2$, was resolved into two fractions but not purified (8), and 4-hydroxyisophthalate hydroxylase, which is responsible for the transformation of 4COOH$_2$ to PCA, was purified and characterized (9). Their genetic determinants, however, are still unavailable. Here we report the cloning and characterization of the *hipH* gene encoding 4-hydroxyisophthalate hydroxylase, which is responsible for the oxidation of 4COOH$_2$ to PCA in 2,4-xylenol catabolism in *P. putida* NCIMB 9866. This fills a gap in our understanding of the gene that encodes a critical step in 2,4-xylenol catabolism.

Received 24 September 2015 **Accepted** 10 November 2015

Accepted manuscript posted online 13 November 2015

Citation Chao H-J, Chen Y-F, Fang T, Xu Y, Huang WE, Zhou N-Y. 2016. HipH catalyzes the hydroxylation of 4-hydroxyisophthalate to protocatechuate in 2,4-xylenol catabolism by *Pseudomonas putida* NCIMB 9866. Appl Environ Microbiol 82:724–731. doi:10.1128/AEM.03105-15.

Editor: R. E. Parales

Address correspondence to Ning-Yi Zhou, n.zhou@pentium.whiov.ac.cn.

Supplemental material for this article may be found at http://dx.doi.org/10.1128/AEM.03105-15.

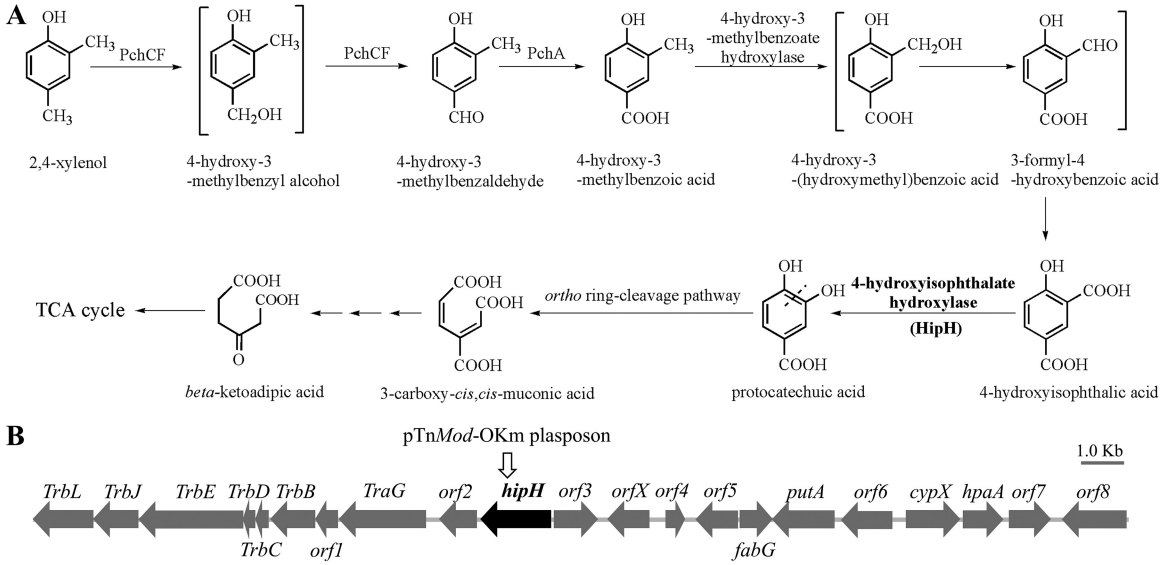

FIG 1 (A) Proposed 2,4-xylenol catabolic pathway of *P. putida* NCIMB 9866 (2, 8, 9) and catabolic reactions catalyzed by PchCF (*p*-cresol methylhydroxylase), PchA (*p*-hydroxybenzaldehyde dehydrogenase), and HipH (4-hydroxyisophthalate hydroxylase) (7). The 4-hydroxy-3-methylbenzoate hydroxylase activity for oxidation of the *ortho*-methyl group of 2,4-xylenol was detected in two fractions from wild-type strain NCIMB 9866 (8). TCA, tricarboxylic acid. (B) Organization of the *hipH* gene cluster obtained by genome walking in both directions from *hipH*. Plasposon pTn*Mod*-OKm was mapped between nucleotides 973 and 974 of the *hipH* gene in mutant Tn94 (open arrow).

MATERIALS AND METHODS

Bacterial strains, plasmids, primers, chemicals, and culture media. The bacterial strains and plasmids used in this study are listed in Table 1, and the primers used are listed in Table 2. *Escherichia coli* was grown aerobically on a rotary shaker (200 rpm) at 37°C in lysogeny broth (LB) or on LB plates with 1.5% (wt/vol) agar. The *Pseudomonas* strains were grown at 30°C in minimal medium (MM) (9) with different carbon sources. The antibiotics were used to supplement the medium at a final concentration of 100 μg ml^{-1} of ampicillin sodium (Amp), 50 μg ml^{-1} of kanamycin sulfate (Kan), or 20 μg ml^{-1} of tetracycline hydrochloride

TABLE 1 Bacterial strains and plasmids used in this study

Strain or plasmid	Characteristic(s)[a] or purpose	Reference or source
P. putida strains		
NCIMB 9866	2,4-Xylenol and *p*-cresol utilizer, Amp^r, Kan^s, Tc^s, wild type	2
NCIMB 9866Δ*hipH*	NCIMB 9866 mutant with *hipH* gene replaced with kanamycin resistance gene from plasposon pTn*Mod*-Okm, Amp^r, Kan^r	This study
NCIMB 9866Δ*hipH*(pRK415-*hipH*)	*hipH* gene complemented by pRK415-*hipH* in NCIMB 9866Δ*hipH*, Amp^r, Kan^r, Tc^r	This study
E. coli strains		
Trans T1	F$^-$ ϕ80(*lacZ*)ΔM15 Δ*lacX74 hsdR*(r_K^- m_K^+) Δ*recA1398 endA1 tonA*	TransGen Biotech
BL21(DE3)	F$^-$ *ompT hsdS*(r_B^- m_B^+) *gal dcm*(DE3)	TransGen Biotech
WM3064	Donor strain for conjugation, 2,6-diaminopimelic acid auxotroph, *thrB1004 pro thi rpsL hsdS lacZ*ΔM15 *RP4-1360* Δ(*araBAD*)*567* Δ*dapA1341*::[*erm pir*(*wt*)]	11
Plasmids		
pET-28a(+)	Expression vector, Kan^r, C/N-terminal His tag/thrombin/T7 tag, T7 *lac* promoter, T7 transcription start, f1 origin, *lacI*	Novagen
pEX18Tc	Gene knockout vector, *oriT*, *sacB*, Tc^r	43
pRK415	Broad-host-range vector, Tc^r	44
pTn*Mod*-OKm	Kan^r, pMB1 replicon, plasposon	10
pET-28a-*hipH*	Expression vector for *hipH* with C-terminal His tag made by cloning *hipH* into NcoI-HindIII restriction site	This study
pET-28a-*pcaHG*	Expression vector for *pcaHG* of *C. glutamicum* made by cloning *pcaHG* into NdeI-HindIII restriction sites	This study
pEX18Tc-*hipH*	*hipH* gene knockout vector containing two DNA fragments homologous to upstream and downstream regions of *hipH* and kanamycin resistance gene from pTn*Mod*-Okm	This study
pRK415-*hipH*	*hipH* gene complementation vector made by fusing *hipH* into HindIII-EcoRI restriction sites of pRK415	This study

[a] Amp^r, resistant to ampicillin; Kan^r, resistant to kanamycin; Tc^r, resistant to tetracycline; Kan^s, sensitive to kanamycin; Tc^s, sensitive to tetracycline.

TABLE 2 Primers used in this study

Primer	Sequence (5′–3′)
BP hipH-01	AGGAGATATACCATGAACAGCATTCAGAGCGTGGACG
BP hipH-02	TGCGGCCGCAAGCTTTGCCAAGGCCTCCATATCGGT
pcagh01	GGAATTCCATATGATGGACATCCCACACTTCGC
pcagh02	CCCAAGCTTGAGTCCAAAAAATGGGGTTTC
KO hipHup-01	ATGATTACGAATTCGCCAGGTACACCACGGGATCTATC
KO hipHup-02	AGAGATTTTGAGACATTCACCTTCTCCGATTTAGCG
KO hipHdown-01	GATGAGTTTTTCTAAAGGCCGCAAGGACATGCAGCT
KO hipHdown-02	GGCCAGTGCCAAGCTTGCAGGGGTCCCCGTCAAATCA
GC hipH-01	TGATTACGCCAAGCTTGATGAACAGCATTCAGAGCGTGG
GC hipH-02	GACGGCCAGTGAATTTCATGCCAAGGCCTCCATATCG
GC hipH-V01	GCAGGAGCGACCATCAGAAGC
GC hipH-V02	ATGACACCGCCTCGCAAGAAG
RThipH01	AACAGCATTCAGAGCGTGGAC
RThipH02	CCCAGGCATGGAAATGCTCC
RTq 16S rDNA-01	TTGACGTTACCGACAGAATAAGC
RTq 16S rDNA-02	GATGCAGTTCCCAGGTTGAGC
Tn-F	TGTCGGGTTTCGCCACCTCTG
Tn-R	CGCATCGGGCTTCCCATACAA

(Tc), as necessary. All of the reagents used were purchased from Aladdin Reagents (Shanghai, China) or Sigma-Aldrich (St. Louis, MO, USA).

Transposon mutagenesis. Transposon mutants of *P. putida* NCIMB 9866 were generated according to a previously reported method (10), with minor modifications. pTn*Mod*-OKm in the donor strain *E. coli* WM3064 (a 2,6-diaminopimelic acid [DAP] auxotroph) (11), previously grown on LB with 0.3 mM DAP, was transferred to strain NCIMB 9866 by conjugation (2:1 donor/recipient ratio; 5 h or overnight mating on an LB agar plate with DAP at 30°C). Mutants containing pTn*Mod*-OKm were selected on LB plates containing Kan and Amp or on MM plates containing 2,4-xylenol, $4COOH_2$, or PCA. Genomic DNA (gDNA) of the mutant strain deficient in 2,4-xylenol utilization was isolated with the TIANamp Bacteria DNA kit (TIANGEN, Beijing, China), and the flanking regions of the insertion site were cloned according to the method previously described (10). Primers Tn-F and Tn-R were used for PCR verification and sequencing of the DNA fragments flanking the transposon insertion site. Genome walking was also conducted to clone the flanking regions of the transposon insertion site by methods described previously (12). The nucleotide sequence was determined by Tsingke Biotech Co. (Wuhan, China). Open reading frames (ORFs) were identified and translated by using the program ORF Finder on the National Center for Biotechnology Information website. The deduced proteins were examined for sequence similarity with other proteins in the GenBank database by using BLAST (13).

Construction of plasmids and strains. DNA manipulation was carried out as described previously (14). The *hipH* gene was PCR amplified with primers BP hipH-01 and BP hipH-02 from the genomic DNA of strain NCIMB 9866 and fused to the NcoI/HindIII restriction sites of pET28a(+) with the In-Fusion HD cloning kit (Clontech, Beijing, China) to produce pET-28a-*hipH*. The *pcaHG* genes encoding PCA-3,4-dioxygenase from *Corynebacterium glutamicum* RES167 (15) were amplified with primers pcagh01 and pcagh02 from its genomic DNA (16) and digested with NdeI and HindIII before being cloned into pET-28a(+) to obtain the expression construct pET-28a-*pcaHG*.

Plasmid pEX18Tc-*hipH* for gene knockout was constructed by fusing PCR products of the kanamycin resistance gene (*kan*) from plasposon pTn*Mod*-OKm, an upstream fragment (uf) of the *hipH* gene amplified with primers KO hipHup-01 and KO hipHup-02, and a downstream fragment (df) amplified with primers KO hipHdown-01 and KO hipHdown-02 to the SacI/HindIII sites of pEX18Tc with the In-Fusion HD cloning kit. The resulting plasmid, with an insert of uf-*kan*-df, was transformed into *E. coli* WM3064 before its conjugation with strain NCIMB 9866 as described previously (11). The double-crossover recombinants of strain NCIMB 9866Δ*hipH* were screened on LB plates containing ampicillin, kanamycin, and 10% (wt/vol) sucrose. Plasmid pRK415-*hipH* for gene complementation was constructed by fusing the PCR product of *hipH*, amplified with primers GC hipH-01 and GC hipH-02, to HindIII- and EcoRI-digested pRK415. It was transformed into *E. coli* WM3064, which was then mated with strain NCIMB 9866Δ*hipH* with *hipH* deleted by conjugation to obtain complemented strain NCIMB 9866Δ*hipH*(pRK415-*hipH*).

RNA preparation and transcription analysis. Strain NCIMB 9866 was grown in MM with 2 mM glucose as a carbon source to an optical density at 600 nm (OD_{600}) of 0.1 and then induced with 2 mM 2,4-xylenol, $4COOH_2$, or succinate for 5 h. Its total RNA was isolated with an RNAprep pure bacterial kit (TIANGEN, Beijing, China) and reverse transcribed into cDNA with a PrimeScript RT Reagent kit with gDNA Eraser (Perfect Real Time) (TaKaRa, Dalian, China). The resulting cDNA was amplified with primers RThipH01 and RThipH02 by real-time quantitative PCR (RT-qPCR) with a CFX Connect Real-Time PCR detection system (Bio-Rad) in a 20-μl reaction mixture volume with iQ SYBR green Supermix (Bio-Rad). All samples were run in triplicate in three independent experiments. Relative expression levels were estimated by the $2^{-\Delta\Delta C_T}$ method, and the 16S rRNA gene was amplified with primers RTq 16S rDNA-01 and RTq 16S rDNA-02 and served as a reference for normalization (17).

Protein purification and analyses. C-terminally His-tagged HipH (HipH-His_6) was expressed in *E. coli* BL21(DE3) carrying pET-28a-*hipH*. N-terminally His-tagged PcaH (His_6-PcaH) and C-terminally His-tagged PcaG (PcaG-His_6) were expressed in *E. coli* BL21(DE3) carrying pET-28a-*pcaHG*. The cells were grown at 37°C to an OD_{600} of 0.4 in LB supplemented with 50 μg ml^{-1} kanamycin. Isopropyl-β-D-thiogalactopyranoside (IPTG) was then added to achieve a final concentration of 0.1 mM, and the culture was incubated at 30°C for another 5 h. HipH-His_6 was purified by Ni^{2+}-nitrilotriacetic acid agarose chromatography (Novagen) and eluted at 200 mM imidazole. Purified recombinant HipH was further dialyzed against imidazole with a Spectra/Por CE dialysis membrane with a molecular weight cutoff of 3,500 (Spectrum Laboratories, Inc., Shanghai, China) at 4°C for 2 days against phosphate buffer (PB) before being stored in glycerol at 4°C. Its purity was monitored by sodium dodecyl sulfate-polyacrylamide gel electrophoresis (SDS-PAGE). All purification procedures were carried out at 4°C, and PB contained 1.0 mM β-mercaptoethanol and was prepared as described previously (9).

Molecular weight determination. Molecular weight was determined by SDS-PAGE and analytical ultracentrifugation.

Analytical ultracentrifugation. The molecular weight of recombinant HipH was determined with an XL-I analytical ultracentrifuge (Beckman Coulter, Fullerton, CA) equipped with a four-cell An-60 Ti rotor. Purified HipH-His_6 (1 mg ml^{-1} in 50 mM PB–1 mM β-mercaptoethanol, pH 7.5) was centrifuged at 4°C at 45,000 × *g* for 12 h with 50 mM PB (1 mM β-mercaptoethanol, pH 7.5) as a control. After ultracentrifugation, data were analyzed by SEDFIT (18).

Enzyme activity assays and intermediate identification. 4-Hydroxyisophthalate hydroxylase (9) and PCA-3,4-dioxygenase (19, 20) activities were determined as previously described. For the assay of $4COOH_2$ hydroxylation by 4-hydroxyisophthalate hydroxylase, the reaction mixture contained 50 mM PB (pH 7.5), 1 mM β-mercaptoethanol, 200 μM NADPH (or NADH), and 200 μM purified HipH-His_6. The reference cuvette contained all of these compounds except the substrate, and the assay was initiated by the addition of 30 μg of $4COOH_2$. The UV spectra at 240 to 400 nM were monitored every minute with a Lambda 25 UV/Vis spectrometer (PerkinElmer, Waltham, MA). For PCA-3,4-dioxygenase activity, cell extracts (30 μg) of *E. coli* BL21(DE3) carrying pET-28a-*pcaHG* were added to the reaction mixture to initiate the hydroxylation of $4COOH_2$ to PCA, and the spectra in the range of 240 to 400 nm were recorded every minute. The molar extinction coefficient for NAD(P)H at 340 nm was 6,220 M^{-1} cm^{-1} (21). One unit of enzyme activity is defined as the amount required for the disappearance (or production) of 1 μmol of substrate (or product)/min at 30°C. Specific activities are expressed in units per milligram of protein.

For time course assays, hydroxylase-catalyzed reactions were carried out with 30-ml reaction mixtures containing 75 μM $4COOH_2$, 300 μM NADPH, and 50 mM PB (pH 7.5). The reaction was initiated by the addition of 400 μg of purified HipH-His_6. One-milliliter samples were withdrawn from the reaction mixture and extracted with equal volumes of ethyl acetate after acidification with HCl. The ethyl acetate layer was collected by centrifugation prior to high-performance liquid chromatography (HPLC) analysis. Identification or quantification of $4COOH_2$ and PCA was done by HPLC and HPLC diode array detector mass spectrometry (HPLC-DAD/MS) as follows.

An Agilent 1200 HPLC system (Agilent Technologies, Palo Alto, CA) equipped with a variable-wavelength detector and an Agilent ZORBAX 300SB-C_{18} column (250 by 4.6 mm [inside diameter], 5-μm particle size) with a column temperature of 30°C was used. The mobile phase consisted of solvents A (0.1% acetic acid in water) and B (methanol). The gradient program started with 20% solvent B, followed by an increase to 50% solvent B from 0 to 8 min, a decrease to 20% solvent B from 8 to 8.1 min, and a steady 20% concentration of solvent B from 8.1 to 12 min. The flow rate was 1.0 ml min^{-1}. The injection volume was 20 μl, and the detection wavelength was 250 nm. Under these conditions, the retention times of $4COOH_2$ and PCA were 4.05 and 2.31 min, respectively. HPLC-DAD/MS analyses were performed as described previously (7).

Identification and quantification of the flavoprotein (flavin adenine dinucleotide [FAD]) present in the fractions taken from the different HipH-His_6 purification steps were determined by HPLC as described previously (22). The retention times of authentic FAD, flavin mononucleotide, and riboflavin were 9.613, 10.547, and 11.717 min, respectively. A calibration curve was generated by injecting known amounts of authentic FAD.

Statistical analysis. Statistical analysis was performed with SPSS version 20.0.0 software. Paired-sample tests were used to calculate probability (*P*) values for the transcription of *hipH*. One-way analysis of variance (ANOVA) was used to calculate *P* values for HipH activity analyses. *P* values of <0.05 and <0.01 were considered statistically significant and highly statistically significant, respectively.

Nucleotide sequence accession number. The GenBank accession number of the nucleotide sequence of the 25,424-bp gene cluster reported in this study is KT428599.

RESULTS

Transposon mutagenesis of *P. putida* NCIMB 9866 for identification of genes responsible for 2,4-xylenol catabolism. To identify the gene coding for 2,4-xylenol catabolism, a pTn*Mod*-OKm plasposon mutant library of *P. putida* NCIMB 9866 was constructed. A library of 9,450 plasposon mutants was screened on MM plates containing PCA or $4COOH_2$ for the desired mutants under the same conditions used to screen the wild-type strain. Two mutants obtained in this way, Tn21 and Tn94, were further tested by MM liquid culture for the ability to grow on 2,4-xylenol or $4COOH_2$ as a sole carbon and energy source. Mutant Tn21 was shown to have lost the ability to use 2,4-xylenol but still grew on 4-hydroxy-3-methylbenzaldehyde. Mutant Tn94 was able to use 2,4-xylenol or $4COOH_2$ as a sole carbon source, but its growth rate was apparently lower than that of the wild-type strain.

From the DNA sequences of the flanking regions of Tn*Mod*-OKm in these two mutant strains, two insertions were mapped in two ORFs, respectively: *orfY* in mutant Tn21 and *orfZ* in mutant Tn94. In mutant Tn21, Tn*Mod*-OKm was mapped between nucleotides 667 and 668 from the start codon of *orfY*, which encodes a 396-amino-acid protein 89% identical (99% query cover) to the cytochrome *c*-type biogenesis protein (CcmI) of *P. putida* GB-1 (GenBank accession number ABY99778) (23). A previous study indicated that *p*-cresol methylhydroxylase contained flavoprotein subunits and cytochrome *c* subunits (24, 25). Mutant Tn21, which is deficient in cytochrome *c*-type synthesis, may then fail to produce a functional *p*-cresol methylhydroxylase in 2,4-xylenol utilization. *orfZ* is 1,635 bp in length, encodes the 544-amino-acid FAD-binding protein monooxygenase, and is 44% identical (28% query cover) to the *iaaM* gene encoding the tryptophan 2-monooxygenase from the tumor-forming plant pathogen *Pseudomonas syringae* pv. savastanoi (GenBank accession number M11035) (26, 27). Since *orfZ* was later found to encode the 4-hydroxyisophthalate hydroxylase involved in 2,4-xylenol degradation, it was designated gene *hipH*. Tn*Mod*-OKm was mapped between nucleotides 973 and 974 (equivalent to residue 325 in the protein sequence) from the start codon of *hipH* in mutant Tn94 (Fig. 1B). Analysis of the HipH conserved domain suggests that an FAD binding domain is at its N terminus, where its coding sequence was disrupted by the transposon insertion in this study. Sequence alignment also indicates that the motifs for FAD and NAD(P)H binding, including GXGXXG, DGXCSXHR, and GXHHLHGDAAHX$_3$PX$_2$GXG XNX$_4$DX$_3$L, which are associated with hydroxylase activity (28, 29), were conserved in HipH in comparison with other FAD-dependent monooxygenases (see Fig. S1 in the supplemental material). It was generally thought that the N-terminal GXGXXG sequence binds the ADP moiety of FAD (30) and amino acids DG of the second motif, DGXCSXHR, are in contact with the riboflavin moiety of FAD (31).

***hipH* is highly transcribed in 2,4-xylenol- and 4-hydroxyisophthalate-induced cells of strain NCIMB 9866.** Previous biochemical characterizations indicate that the 4-hydroxyisophthalate hydroxylase activity for $4COOH_2$ catabolism was induced by the presence of 2,4-xylenol or $4COOH_2$ (9). In the present study, the transcriptional level of *hipH* was further analyzed by RT-qPCR. As shown in Fig. S2 in the supplemental material, the level of *hipH* mRNA expression was 8.4 times as high in 2,4-xylenol-grown cells and 8.1 times as high in $4COOH_2$-grown cells as in succinate-grown cells. This is con-

TABLE 3 Comparative analysis of 4-hydroxyisophthalate hydroxylase previously reported[d] and HipH in this study

Enzyme characteristic	4-Hydroxyisophthalate hydroxylase	HipH
Mol wt (10^3)[a]	56–57	62.9
Mol mass (kDa)[b]	110	103
Subunit structure	Dimer	Dimer
K_m (μM)		
NADH	105	72.76 ± 12.06
NADPH	71	64.31 ± 13.16
$4COOH_2$	42	11.40 ± 3.05[c]
FAD (mol/mol)	1	0.79
pH optimum	8	7.5
Inhibition of chloride ions	Yes	Yes
Substrate	$4COOH_2$, 5-sulfosalicylate	$4COOH_2$, 5-sulfosalicylate

[a] Determined by SDS-PAGE.
[b] Determined by analytical ultracentrifugation.
[c] With NADPH as a cofactor.
[d] In reference 9.

sistent with the previous observation of 2,4-xylenol- or $4COOH_2$-induced 4-hydroxyisophthalate hydroxylase activity (9). The result showed that the *hipH* gene was likely involved in the catabolism of 2,4-xylenol.

***hipH* is essential for 2,4-xylenol catabolism in strain NCIMB 9866.** To further test whether *hipH* is involved in the 2,4-xylenol metabolism of strain NCIMB 9866, both knockout and complemented strains were constructed. Strain NCIMB 9866Δ*hipH* was no longer able to grow with 2,4-xylenol, 4-hydroxy-3-methylbenzoate, or $4COOH_2$ as a sole carbon and energy source. However, it was still capable of growing on *p*-cresol, 4-hydroxybenzoate, or PCA. On the other hand, complemented strain NCIMB 9866Δ*hipH*(pRK415-*hipH*) regained the ability to grow on 2,4-xylenol, 4-hydroxy-3-methylbenzoate, or $4COOH_2$. These results clearly indicated that the *hipH* gene is essential for the catabolism of 2,4-xylenol in strain NCIMB 9866 and HipH is likely the enzyme that catalyzes the hydroxylation of $4COOH_2$ to PCA.

Purification and biochemical properties of HipH. *hipH*, which encodes a 544-amino-acid FAD-binding protein monooxygenase, was cloned into pET28a(+) to produce a polypeptide with a His tag fused at the C terminus of HipH (HipH-His_6). A total of 5.9 mg of recombinant HipH-His_6 with a specific activity of 1.54 U mg protein^{-1} against 4-hydroxyisophthalate was purified from 200 ml of culture.

Purified recombinant HipH has a molecular mass of approximately 62.9 kDa and consists of a single polypeptide as observed by SDS-PAGE (see Fig. S3 in the supplemental material). As deduced from analytical ultracentrifugation, the molecular mass of HipH was approximately 110 kDa, suggesting that it is likely a dimer. The molecular weight of HipH-His_6 in the present study is virtually the same as that in the previous literature, as determined by the sedimentation equilibrium method and SDS-PAGE (9) (Table 3). As shown in Table 4, kinetic assays revealed that the K_m value (11.40 ± 3.05 μM) of HipH-His_6 for $4COOH_2$ with NADPH was almost the same as that with NADH (11.23 ± 2.43 μM). In terms of k_{cat}/K_m values, the catalytic efficiency of HipH-His_6 for $4COOH_2$ with NADPH (10.55 ± 2.24 μM^{-1} min^{-1}) was similar to that with NADH (11.28 ± 1.81 μM^{-1} min^{-1}). However, the K_m value of the 4-hydroxyisophthalate hydroxylase purified from strain NCIMB 9866 for $4COOH_2$ (9) is higher than that of HipH-His_6 in this study. The two cofactors have similar affinities for HipH-His_6 purified in this study, with apparent K_m values of 64.31 ± 13.16 μM for NADPH and 72.76 ± 12.06 μM for NADH (Table 4), which are slightly different from those for the 4-hydroxyisophthalate hydroxylase purified from strain NCIMB 9866 (9) (Table 3), respectively.

The sequence alignment described above indicated that HipH contains an FAD domain, and it was also evidenced by the yellow-brown color of purified HipH-His_6. The presence of FAD in HipH-His_6 was confirmed by its absorption maxima at 375 and 450 nm, as well as its retention time (9.613 min), which is the same as that of authentic FAD, in HPLC analysis. Quantification analysis showed that purified HipH-His_6 contained 0.79 mol of FAD/mol of protein, suggesting that 1 mol of HipH contains approximately 1 mol of FAD. When the FAD concentrations were 0.5, 1, 5, and 50 times that of HipH-His_6, the catalytic activity was not evidently changed, suggesting that FAD was tightly bound to HipH. This is similar to the native 4-hydroxyisophthalate hydroxylase purified from strain NCIMB 9866, which also contained 1 mol of FAD/mol of protein (9).

Interestingly, the HipH-His_6 activity for $4COOH_2$ had different pH optima in the following buffers: pH 7.5 in 50 mM PB (with a specific activity of 1.54 U mg^{-1}), pH 7.0 in 50 mM Tris-H_2SO_4 buffer (0.99 U mg^{-1}), and 50 mM in Tris-HCl buffer (0.64 U mg^{-1}). The maximal specific activity of HipH-His_6 for $4COOH_2$ was obtained at pH 7.5 in 50 mM PB. These are different from those of the 4-hydroxyisophthalate hydroxylase purified from strain NCIMB 9866 (9) (Table 3). As shown in Fig. S4 in the supplemental material, the enzyme activity decreased significantly with an increase in the chloride ion level, which was consistent with a previously report (9). Many flavoprotein hydroxylases have been reported to be inhibited by chloride ions, such as 3-hydroxyphenylacetate 6-hydroxylase (32) and 3-hydroxybenzoate 6-hydroxylase (33). It was generally thought that negatively charged chlorine could interfere with the binding and/or reactivity of the enzyme with oxygen, NADH, or both.

TABLE 4 Kinetic parameters of recombinant HipH on 4-hydroxyisophthalate with NADPH or NADH as a cofactor[a]

Substrate	Cofactor	K_m (μM)	k_{cat} (min^{-1})	k_{cat}/K_m (μM^{-1} min^{-1})
4-Hydroxyisophthalate	NADPH	11.40 ± 3.05	120.24 ± 8.73	10.55 ± 2.24
4-Hydroxyisophthalate	NADH	11.23 ± 2.43	126.65 ± 8.15	11.28 ± 1.81
NADPH		64.31 ± 13.16		
NADH		72.76 ± 12.06		

[a] The kinetic constants were calculated by nonlinear regression analysis, and the values are expressed as means ± standard deviations ($n = 4$). k_{cat} values were calculated on the basis of a subunit M_r of 62,890. There was a significant difference in the activity of recombinant HipH on $4COOH_2$ with NADPH or NADH as a cofactor ($P < 0.001$, one-way ANOVA).

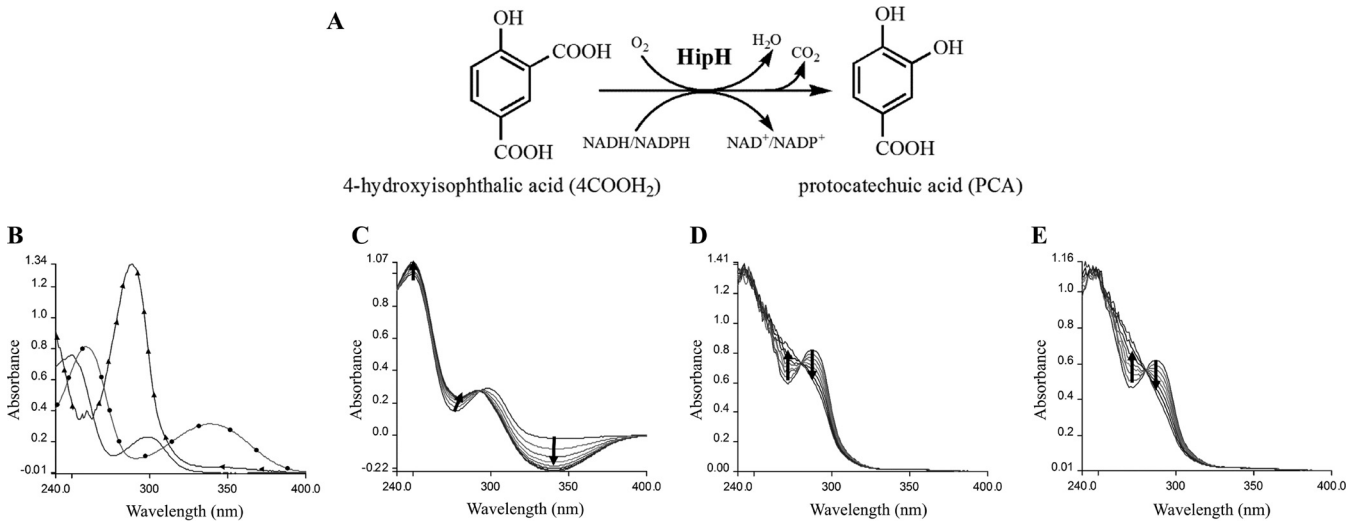

FIG 2 Determination of *hipH*-encoded 4-hydroxyisophthalate hydroxylase activity. (A) Proposed conversion of $4COOH_2$ to PCA catalyzed by HipH. (B) Absorption spectra of authentic $4COOH_2$ (—), PCA (▲), and NADPH (●). (C) Spectrophotometric changes during the hydroxylation of $4COOH_2$ by *hipH*-encoded 4-hydroxyisophthalate hydroxylase. (D) Transformation of the product of HipH-His_6-catalyzed hydroxylation of $4COOH_2$ by cell extracts (30 μg) of *E. coli* BL21(DE3) carrying pET-28a-*pcaHG* with PCA-3,4-dioxygenase. (E) Ring cleavage of authentic PCA catalyzed by cell extracts of *E. coli* BL21(DE3) carrying pET-28a-*pcaHG*.There is no enzyme activity in the negative control, *E. coli* BL21(DE3)/pET-28a(+), for any of the above three reactions in panels C, D, and E. The arrows indicate the directions of spectral changes.

HipH catalyzes the NADH- and NADPH-dependent hydroxylation of 4-hydroxyisophthalate to PCA. Previously, PCA was confirmed as the product of $4COOH_2$ oxidation catalyzed by the 4-hydroxyisophthalate hydroxylase purified from 2,4-xylenol-grown strain NCIMB 9866 only by spectrophotometry, with a maximum absorbance at 290 nm (9, 19). In the present study, the incubation of HipH-His_6 with $4COOH_2$ and NAPH was also found by spectrophotometry to have resulted in the accumulation of a product (λ_{max}, 290 nm) (Fig. 2C) together with the consumption of NADPH (λ_{max}, 340 nm). Subsequently, cell extracts containing PcaGH (PCA-3,4-dioxygenase) expressed in *E. coli* BL21(DE3)/pET-28a-*pcaHG* converted both the above-described product of HipH-His_6-catalyzed $4COOH_2$ hydroxylation and authentic PCA to 3-carboxy-*cis*,*cis*-muconate (λ_{max}, 270 nm) (Fig. 2D and E). On the other hand, HPLC analysis of $4COOH_2$ hydroxylation by HipH-His_6 showed that the substrate $4COOH_2$ gradually decreased (retention time of 4.05 min) and the PCA chromatographic peak gradually increased (2.31 min) in the presence of NADPH (see Fig. S5A in the supplemental material). The product with a retention time of 2.31 min was further confirmed as PCA with a stable deprotonated ion of $(M - H)^-$ (m/z = 152.97) in its mass spectrum (see Fig. S5B). The same product was reported from the conversion of $4COOH_2$ by purified 4-hydroxyisophthalate hydroxylase (9) but by thin-layer and paper chromatography methods. In a time course assay of HipH-His_6-catalyzed hydroxylation, $4COOH_2$ consumption (74.3 μM) was equivalent to the total accumulation of PCA (74.1 μM) (Fig. 3), indicating complete conversion of $4COOH_2$ to PCA. These results clearly indicate that HipH catalyzed the hydroxylation of $4COOH_2$ to yield PCA.

Substrate specificity of purified HipH-His_6. The substrate specificity of purified HipH-His_6 for $4COOH_2$ and other structurally similar compounds was tested by spectrophotometric assay. Substrate-dependent oxidation of NADPH catalyzed by HipH-His_6 was detected with $4COOH_2$ (with an activity of 1.54 ± 0.09 U mg protein^{-1}) and 5-sulfosalicylate (0.10 ± 0.04 U mg protein^{-1}) as substrates. No activity against salicylate, 3-hydroxybenzoate, 4-hydroxy-3-methylbenzoate, 4-hydroxy-3-nitrobenzoate, vanillate, 2,5-dihydroxybenzoate, 2,4-dihydroxybenzoate, 3,4-dihydroxybenzoate, phthalate, isophthalate, terephthalate, 3-formyl-4-hydroxybenzoate, or L-tryptophan was detected. This is same as the aromatic substrate specificity of 4-hydroxyisophthalate hydroxylase previously reported (9). As stated above, the closest homolog of HipH is IaaM, which catalyzes the monooxygenation of L-tryptophan, but it was not a substrate for HipH in this study. On the other hand, it had no catalytic activity for 4-hydroxybenzoate, which was the precursor of the ring cleavage substrate PCA in the *p*-cresol metabolic pathway (34, 35). This suggests that the hydroxylases for this step of 2,4-xylenol and *p*-cresol catabolism are different.

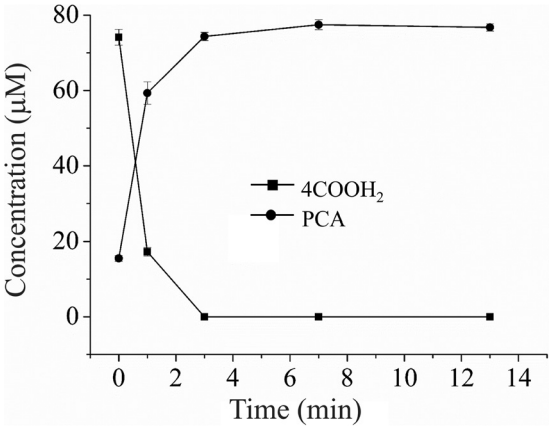

FIG 3 Time course of 4-hydroxyisophthalate hydroxylation catalyzed by HipH with NADH as the cofactor monitored by HPLC.

DISCUSSION

p-Cresol metabolism has been reported in a number of bacterial strains, including *Pseudomonas* sp. (1), *P. putida* NCIMB 9866 (24, 34, 35), *P. putida* NCIMB 9869 (34, 36), *P. mendocina* KR1 (37), and *Corynebacterium glutamicum* (38). However, *P. putida* NCIMB 9866 is the only reported strain capable of growing aerobically on 2,4-xylenol as a sole carbon and energy source (2). Thus, strain NCIMB 9866 is a unique candidate for studying the catabolism of both 2,4-xylenol and *p*-cresol. In this strain, the oxidation of a *para*-methyl group to a carboxyl group in both *p*-cresol and 2,4-xylenol is catalyzed by the same set of enzymes, PchCF and PchA (7), but the subsequent catabolism of these two compounds occurred via different routes and was catalyzed by different enzymes. After the initial oxidation in *p*-cresol catabolism, 4-hydroxybenzoate was formed via two intermediates of 4-hydroxybenzyl alcohol and 4-hydroxybenzaldehyde, which is directly converted to PCA by 4-hydroxybenzoate hydroxylase (24, 35). For 2,4-xylenol catabolism, the *ortho*-methyl group of 4-hydroxy-3-methylbenzoate newly formed from the initial oxidation is further oxidized to a carboxyl group to form $4COOH_2$ by 4-hydroxy-3-methylbenzoate hydroxylase (8) before being converted to PCA by 4-hydroxyisophthalate hydroxylase (9) (Fig. 1A). In this study, the *hipH* gene, which encodes 4-hydroxyisophthalate hydroxylase in 2,4-xylenol catabolism, has been cloned by transposon mutagenesis and the purified HipH-His_6 catalyzed the hydroxylation of $4COOH_2$ to PCA. That the *hipH* deletion-carrying strain was unable to grow on 2,4-xylenol, 4-hydroxy-3-methylbenzoate, or $4COOH_2$ but was able to grow on PCA clearly indicates that the previous proposed pathway (shown in Fig. 1A) is reasonably correct. However, this deletion has no impact on the *p*-cresol catabolic pathway. These observations confirmed that the catabolism of 2,4-xylenol and *p*-cresol into PCA occurred through independent pathways of 4-hydroxy-3-methylbenzoate and 4-hydroxybenzoate, respectively. This fills a gap in our understanding of the gene that encodes a critical step in the biodegradation of 2,4-xylenol and also provides another example of biochemical and genetic diversity of the microbial catabolism of structurally similar compounds.

From the proposed catabolic pathway of 2,4-xylenol in *P. putida* NCIMB 9866, the gene that encodes 4-hydroxy-3-methylbenzoate hydroxylase, which catalyzes the hydroxylation of 4-hydroxy-3-methylbenzoate, is still missing and the enzyme has not been purified either. Thus, efforts to find the other genes responsible for the lower catabolic pathway were also made by using a genome walking assay. Subsequently, a 25,424-bp DNA fragment extending from the *hipH* gene was obtained and sequenced as outlined in Fig. 1B. Twenty-one ORFs were annotated on the basis of BLAST analysis. The upstream region of this fragment containing the genes *trbBCDEJL* and *traG* is proposed to encode inner membrane conjugal transfer proteins of the F sex factor (39). Orf2 is most similar (99% identity) to the D-alanyl–D-alanine endopeptidase from *Comamonas testosteroni* (KGG85579). OrfX is most similar (62% identity) to the putative MetA pathway of phenol degradation by *C. testosteroni* TA441 (BAA88498) (40). FabG is most similar (47% identity) to the short-chain dehydrogenase/reductase from *Hydrogenophaga intermedia* (CDN90408). PutA is most similar (49% identity) to the NAD-dependent aldehyde dehydrogenase of *Celeribacter indicus* P73 (AJE49484) (41). Orf6 is most similar (55% identity) to the putative ferredoxin-NAD(+) reductase of *Azospirillum brasilense* Sp245 (CCD02733) (42). Nevertheless, no candidates were found to possibly encode the enzymes involved in the transformation of the *ortho*-methyl group of 2,4-xylenol. Such genes were not found in the cluster containing the *pchACF* genes for the oxidation of the *para*-methyl group of 2,4-xylenol either in a previous study (7). Therefore, it is quite possible that structural genes for 2,4-xylenol utilization were spread between a plasmid and the chromosome in strain NCIMB 9866. Further work is under way to clarify the entire 2,4-xylenol metabolic pathway of this strain at the genetic and biochemical levels.

ACKNOWLEDGMENTS

We are grateful to the Core Facility and Technical Support in the Wuhan Institute of Virology, Chinese Academy of Sciences.

FUNDING INFORMATION

National Key Basic Research Program of China (973 Program) provided funding to Ning-Yi Zhou under grant number 2012CB725202. National Natural Science Foundation of China (NSFC) provided funding to Hong-Jun Chao under grant number 31400068. National Natural Science Foundation of China (NSFC) provided funding to Ti Fang under grant number 31400114. State Key Laboratory of Microbial Metabolism, Shanghai Jiao Tong University provided funding to Hong-Jun Chao under grant number MMLKF15-05.

REFERENCES

1. **Dagley S, Patel MD.** 1957. Oxidation of *p*-cresol and related compounds by a *Pseudomonas*. Biochem J **66:**227–233. http://dx.doi.org/10.1042/bj0660227.
2. **Chapman PJ, Hopper DJ.** 1968. The bacterial metabolism of 2,4-xylenol. Biochem J **110:**491–498. http://dx.doi.org/10.1042/bj1100491.
3. **Rudolphi A, Tschech A, Fuchs G.** 1991. Anaerobic degradation of cresols by denitrifying bacteria. Arch Microbiol **155:**238–248. http://dx.doi.org/10.1007/BF00252207.
4. **Hinteregger C, Leitner R, Loidl M, Ferschl A, Streichsbier F.** 1992. Degradation of phenol and phenolic compounds by *Pseudomonas putida* EKII. Appl Microbiol Biotechnol **37:**252–259. http://dx.doi.org/10.1007/BF00178180.
5. **Pieper DH, Engesser KH, Knackmuss H-J.** 1990. (+)-4-Carboxymethyl-2,4-dimethylbut-2-en-4-olide as dead-end metabolite of 2,4-dimethylphenoxyacetic acid or 2,4-dimethylphenol by *Alcaligenes eutrophus* JMP 134. Arch Microbiol **154:**600–604. http://dx.doi.org/10.1007/BF00248843.
6. **Pieper DH, Stadlerfritzsche K, Knackmuss HJ, Timmis KN.** 1995. Formation of dimethylmuconolactones from dimethylphenols by *Alcaligenes eutrophus* JMP 134. Appl Environ Microbiol **61:**2159–2165.
7. **Chen YF, Chao HJ, Zhou NY.** 2014. The catabolism of 2,4-xylenol and *p*-cresol share the enzymes for the oxidation of *para*-methyl group in *Pseudomonas putida* NCIMB 9866. Appl Microbiol Biotechnol **98:**1349–1356. http://dx.doi.org/10.1007/s00253-013-5001-z.
8. **El-Mansi EMT, Hopper DJ.** 1990. Resolution of the 4-hydroxy-3-methylbenzoate hydroxylase of *Pseudomonas putida* into two protein components. FEMS Microbiol Lett **66:**147–152. http://dx.doi.org/10.1111/j.1574-6968.1990.tb03987.x.
9. **Elmorsi EA, Hopper DJ.** 1977. The purification and properties of 4-hydroxyisophthalate hydroxylase from *Pseudomonas putida* NCIB 9866. Eur J Biochem **76:**197–208. http://dx.doi.org/10.1111/j.1432-1033.1977.tb11585.x.
10. **Dennis JJ, Zylstra GJ.** 1998. Plasposons: modular self-cloning minitransposon derivatives for rapid genetic analysis of Gram-negative bacterial genomes. Appl Environ Microbiol **64:**2710–2715.
11. **Saltikov CW, Newman DK.** 2003. Genetic identification of a respiratory arsenate reductase. Proc Natl Acad Sci U S A **100:**10983–10988. http://dx.doi.org/10.1073/pnas.1834303100.
12. **Siebert PD, Chenchik A, Kellogg DE, Lukyanov KA, Lukyanov SA.** 1995. An improved PCR method for walking in uncloned genomic DNA. Nucleic Acids Res **23:**1087–1088. http://dx.doi.org/10.1093/nar/23.6.1087.
13. **Altschul SF, Madden TL, Schaffer AA, Zhang JH, Zhang Z, Miller W,**

Lipman DJ. 1997. Gapped BLAST and PSI-BLAST: a new generation of protein database search programs. Nucleic Acids Res **25:**3389–3402. http://dx.doi.org/10.1093/nar/25.17.3389.
14. **Sambrook J, Russell DW.** 2001. Molecular cloning: a laboratory manual, 3rd ed. Cold Spring Harbor Laboratory Press, Cold Spring Harbor, NY.
15. **Shen X, Liu S.** 2005. Key enzymes of the protocatechuate branch of the beta-ketoadipate pathway for aromatic degradation in *Corynebacterium glutamicum*. Sci China C Life Sci **48:**241–249. http://dx.doi.org/10.1007/BF03183617.
16. **Tauch A, Kirchner O, Loffler B, Gotker S, Puhler A, Kalinowski J.** 2002. Efficient electrotransformation of *Corynebacterium diphtheriae* with a mini-replicon derived from the *Corynebacterium glutamicum* plasmid pGA1. Curr Microbiol **45:**362–367. http://dx.doi.org/10.1007/s00284-002-3728-3.
17. **Livak KJ, Schmittgen TD.** 2001. Analysis of relative gene expression data using real-time quantitative PCR and the $2^{-\Delta\Delta C_T}$ method. Methods **25:**402–408. http://dx.doi.org/10.1006/meth.2001.1262.
18. **Schuck P.** 2000. Size-distribution analysis of macromolecules by sedimentation velocity ultracentrifugation and Lamm equation modeling. Biophys J **78:**1606–1619. http://dx.doi.org/10.1016/S0006-3495(00)76713-0.
19. **Stanier RY, Ingraham JL.** 1954. Protocatechuic acid oxidase. J Biol Chem **210:**799–808.
20. **Gross SR, Gafford RD, Tatum EL.** 1956. The metabolism of protocatechuic acid by Neurospora. J Biol Chem **219:**781–796.
21. **Zhou NY, Fuenmayor SL, Williams PA.** 2001. *nag* genes of *Ralstonia* (formerly *Pseudomonas*) sp. strain U2 encoding enzymes for gentisate catabolism. J Bacteriol **183:**700–708. http://dx.doi.org/10.1128/JB.183.2.700-708.2001.
22. **Miramar MD, Costantini P, Ravagnan L, Saraiva LM, Haouzi D, Brothers G, Penninger JM, Peleato ML, Kroemer G, Susin SA.** 2001. NADH oxidase activity of mitochondrial apoptosis-inducing factor. J Biol Chem **276:**16391–16398. http://dx.doi.org/10.1074/jbc.M010498200.
23. **de Vrind JPM, Brouwers GJ, Corstjens PLAM, den Dulk J, de Vrind-de Jong EW.** 1998. The cytochrome *c* maturation operon is involved in manganese oxidation in *Pseudomonas putida* GB-1. Appl Environ Microbiol **64:**3556–3562.
24. **Kim JH, Fuller JH, Cecchini G, McIntire WS.** 1994. Cloning, sequencing, and expression of the structural genes for the cytochrome and flavoprotein subunits of *p*-cresol methylhydroxylase from two strains of *Pseudomonas putida*. J Bacteriol **176:**6349–6361.
25. **McIntire W, Hopper DJ, Singer TP.** 1985. *p*-Cresol methylhydroxylase. Assay and general properties. Biochem J **228:**325–335. http://dx.doi.org/10.1042/bj2280325.
26. **Yamada T, Palm CJ, Brooks B, Kosuge T.** 1985. Nucleotide-sequences of the *Pseudomonas savastanoi* indoleacetic-acid genes show homology with Agrobacterium tumefaciens T-DNA. Proc Natl Acad Sci U S A **82:**6522–6526. http://dx.doi.org/10.1073/pnas.82.19.6522.
27. **Gaweska HM, Taylor AB, Hart PJ, Fitzpatrick PF.** 2013. Structure of the flavoprotein tryptophan 2-monooxygenase, a key enzyme in the formation of galls in plants. Biochemistry **52:**2620–2626. http://dx.doi.org/10.1021/bi4001563.
28. **Eppink MHM, Schreuder HA, VanBerkel WJH.** 1997. Identification of a novel conserved sequence motif in flavoprotein hydroxylases with a putative dual function in FAD/NAD(P)H binding. Protein Sci **6:**2454–2458. http://dx.doi.org/10.1002/pro.5560061119.
29. **van Berkel WJH, Kamerbeek NM, Fraaije MW.** 2006. Flavoprotein monooxygenases, a diverse class of oxidative biocatalysts. J Biotechnol **124:**670–689. http://dx.doi.org/10.1016/j.jbiotec.2006.03.044.
30. **Wierenga RK, Terpstra P, Hol WGJ.** 1986. Prediction of the occurrence of the ADP-binding beta-alpha-beta-fold in proteins, using an amino-acid-sequence fingerprint. J Mol Biol **187:**101–107. http://dx.doi.org/10.1016/0022-2836(86)90409-2.
31. **Eggink G, Engel H, Vriend G, Terpstra P, Witholt B.** 1990. Rubredoxin reductase of *Pseudomonas oleovorans*: structural relationship to other flavoprotein oxidoreductases based on one NAD and two FAD fingerprints. J Mol Biol **212:**135–142. http://dx.doi.org/10.1016/0022-2836(90)90310-I.
32. **Van Berkel WJ, Van Den Tweel WJ.** 1991. Purification and characterisation of 3-hydroxyphenylacetate 6-hydroxylase: a novel FAD-dependent monooxygenase from a *Flavobacterium* species. Eur J Biochem **201:**585–592. http://dx.doi.org/10.1111/j.1432-1033.1991.tb16318.x.
33. **Montersino S, Orru R, Barendregt A, Westphal AH, van Duijn E, Mattevi A, van Berkel WJH.** 2013. Crystal structure of 3-hydroxybenzoate 6-hydroxylase uncovers lipid-assisted flavoprotein strategy for regioselective aromatic hydroxylation. J Biol Chem **288:**26235–26245. http://dx.doi.org/10.1074/jbc.M113.479303.
34. **Cronin CN, Kim J, Fuller JH, Zhang XP, McIntire WS.** 1999. Organization and sequences of *p*-hydroxybenzaldehyde dehydrogenase and other plasmid-encoded genes for early enzymes of the *p*-cresol degradative pathway in *Pseudomonas putida* NCIMB 9866 and 9869. DNA Seq **10:**7–17. http://dx.doi.org/10.3109/10425179909033930.
35. **Hopper DJ.** 1976. The hydroxylation of *p*-cresol and its conversion to *p*-hydroxybenzaldehyde in *Pseudomonas putida*. Biochem Biophys Res Commun **69:**462–468. http://dx.doi.org/10.1016/0006-291X(76)90544-1.
36. **Keat MJ, Hopper DJ.** 1978. *p*-Cresol and 3,5-xylenol methylhydroxylases in *Pseudomonas putida* NCIB 9869. Biochem J **175:**649–658. http://dx.doi.org/10.1042/bj1750649.
37. **Whited GM, Gibson DT.** 1991. Separation and partial characterization of the enzymes of the toluene-4-monooxygenase catabolic pathway in *Pseudomonas mendocina* KR1. J Bacteriol **173:**3017–3020.
38. **Li T, Chen X, Chaudhry MT, Zhang B, Jiang CY, Liu SJ.** 2014. Genetic characterization of 4-cresol catabolism in *Corynebacterium glutamicum*. J Biotechnol **192:**355–365. http://dx.doi.org/10.1016/j.jbiotec.2014.01.017.
39. **Frost LS, Ippen-Ihler K, Skurray RA.** 1994. Analysis of the sequence and gene products of the transfer region of the F sex factor. Microbiol Rev **58:**162–210.
40. **Arai H, Ohishi T, Chang MY, Kudo T.** 2000. Arrangement and regulation of the genes for *meta*-pathway enzymes required for degradation of phenol in *Comamonas testosteroni* TA441. Microbiology **146:**1707–1715. http://dx.doi.org/10.1099/00221287-146-7-1707.
41. **Cao J, Lai Q, Yuan J, Shao Z.** 2015. Genomic and metabolic analysis of fluoranthene degradation pathway in *Celeribacter indicus* P73T. Sci Rep **5:**7741. http://dx.doi.org/10.1038/srep07741.
42. **Wisniewski-Dyé F, Borziak K, Khalsa-Moyers G, Alexandre G, Sukharnikov LO, Wuichet K, Hurst GB, McDonald WH, Robertson JS, Barbe V, Calteau A, Rouy Z, Mangenot S, Prigent-Combaret C, Normand P, Boyer M, Siguier P, Dessaux Y, Elmerich C, Condemine G, Krishnen G, Kennedy I, Paterson AH, Gonzalez V, Mavingui P, Zhulin IB.** 2011. Azospirillum genomes reveal transition of bacteria from aquatic to terrestrial environments. PLoS Genet **7:**e1002430. http://dx.doi.org/10.1371/journal.pgen.1002430.
43. **Hoang TT, Karkhoff-Schweizer RR, Kutchma AJ, Schweizer HP.** 1998. A broad-host-range Flp-FRT recombination system for site-specific excision of chromosomally-located DNA sequences: application for isolation of unmarked *Pseudomonas aeruginosa* mutants. Gene **212:**77–86. http://dx.doi.org/10.1016/S0378-1119(98)00130-9.
44. **Keen NT, Tamaki S, Kobayashi D, Trollinger D.** 1988. Improved broad-host-range plasmids for DNA cloning in Gram-negative bacteria. Gene **70:**191–197. http://dx.doi.org/10.1016/0378-1119(88)90117-5.